

## COMPARISON OF PREDICTIONS BY MCNP AND EGSNRC OF RADIATION DOSE IMPARTED TO VARIOUS MATERIAL TARGETS BY BEAMS AND SMALL VOLUMETRIC SOURCES.

Eric Steinfelds  
Department of Nuclear and Radiological Engineering  
University of Florida  
Gainesville, Florida  
[steinfel@earthlink.net](mailto:steinfel@earthlink.net)

### ABSTRACT

EGSnrc is optimized in order to model the transport of electrons in a significantly more time efficient manner than MCNP. However, it seems that direct electron contributions to dose are easier to trace and record with MCNP than with EGSnrc. MCNP makes it clear where the electrons stop and where secondary photons continue for e-beam simulations. Within the processing algorithms of EGSnrc, photon dosimetry and electron dosimetry are intermixed and very difficult to separate. The rad transport expert would wonder why EGSnrc reports small contributions from beta particles which penetrate well beyond the max CDSA range of the beta, until one considers that EGSnrc models and records beta electron and secondary photon doses simultaneously. For the nuclear engineer, it is *also* instructive to point out that EGSnrc is designed exclusively for the transport of photons and electrons(+/-), not for hadrons (i.e. protons, alphas, etc.). This is rather limiting in versatility for EGSnrc compared to MCNPX, which now does include many hadrons in addition to alphas. The predominant modes of radiation therapy are still done with hard photons, semi-hard photons, and less frequently with energetic electrons; either from accelerators or radioisotopic sources (e.g. Ir-192 etc.). Radiographic imaging relies on positrons, photons, and occasionally neutrons. Thus, EGSnrc is versatile enough with its choices of radiative particles for para-clinical applications. For geometric configurations and designs in the medical realm, virtually all material samples and targets are arranged within rectangular voxels, whose planar boundaries are aligned with their respective x,y, and z axes. While this might seem very limiting to the traditional nuclear engineering oriented user of MCNP, this is quite sufficient for the medical physicists and medical physics developers, who almost always work with 3 dimensional images of patients which are mapped as voxels with a grid-partitioning of often more than 70 by 70 by 50. These mappings of the densities and the images are recorded as files which are translated from the CT image files of a given patient or specimen. In this paper, it is the simulated doses imparted to each voxel of a given geometry that are recorded and reviewed.

**KEYWORDS:** MCNP, EGSnrc, dosimetry, dosimetric comparison, rectangular beam.

### 1. INTRODUCTION

These computational dose estimates were generated by both MCNP and EGSnrc in order to be reviewed for similarities and differences of performances between that of the two Monte Carlo codes. EGSnrc was developed by the Research Center of Canada.[1] Dose per voxel is emphasized in this paper because medical physicists are mostly interested in doses resulting from radiation, and not very much in the transmissions of particles. Note that the two computers used

for respective comparisons between MCNP and EGSnrc are both Dells with the single Intel Pentium(R) 4M CPU.

More most of this paper, a square collimated beam of some particle is modelled. This beam is transversely shaped as a square whose length of a side is 1.6 cm. Within this paper, the target of such a beam is a cubic water-like material. The beam targets the middle of this 'soft tissue'. The objective is to compare the time durations, the ease of operation, plausibility of results, and degree of agreement of results between MCNP and EGSnrc.

The simulation results between MCNP and EGSnrc are similar but not identical. Among preliminary examples of simulation for a given setup of water (or flesh equivalent) filled voxels which are irradiated by rectangular beams of either photons or electrons, it was generally found at almost all energy levels (.5 thru 18MeV) that EGSnrc predicts slightly higher doses than MCNP does. These are the doses imparted to samples within the target and to the material regions surrounding the target. It is a major aid to do MCNP modelling in pure photon mode and separately in (photon,electron) mode in order to effectively account for the dose contributions from secondary electrons. It will become apparent in the first table that MCNP models primary photons and scattered photons from primary photons (and possibly tertiary photons) almost as fast as EGSnrc does, but EGSnrc is at least 20 % at lower energies. For energies above 5MeV, the discrepancy in dose predictions within the first 3 centimeters of beam penetration leads to predictions by EGSnrc which are more than 10 percent larger than the MCNP predictions. The same number of source particles was used in each simulation, per geometrical target. For simulations of electron beam, the speed advantage of EGSnrc per number of source particles is rather extreme, where the EGSnrc is easily an order of magnitude faster, even approaching a 50 fold speed advantage.

Some therapy uses radio-seed implants and various styles of stereotactic radiotherapy. In addition to modelling rectangular beam, a brief example of comparison is also given of a point source emitting the 'strong'  $\gamma$ -ray of Cs-137 toward the end of this text, including a figure (4).

## **2. METHOD, GEOMETRIES PICKED, AND INPUT FOR MC MODELLING**

For most of the examples a rectangular structure of flesh equivalent material or H<sub>2</sub>O could be described as being bombarded by mono-energetic beams of electrons and photons. One example is given of a spherically symmetrical phantom with 18 cm diameter being irradiated by the main gamma ray (i.e. .662 MeV) from a Cs-137 point source. The gamma ray instigated dose predicted (by MCNP and EGSnrc) to voxels as a function of radial distance are given in the last table at the end of this paper.

Let us consider a perfectly collimated rectangular beam pointing along the x-axis hitting a rectangular block which has been subdivided into 6 by 5 by 3 voxels. Along the x-axis, there are 6 successive voxels of H<sub>2</sub>O. Figure (1) illustrates the geometry. The red arrows denote the beam of primary electrons or photons. See figure (1):

## Geometry of beam simulations:

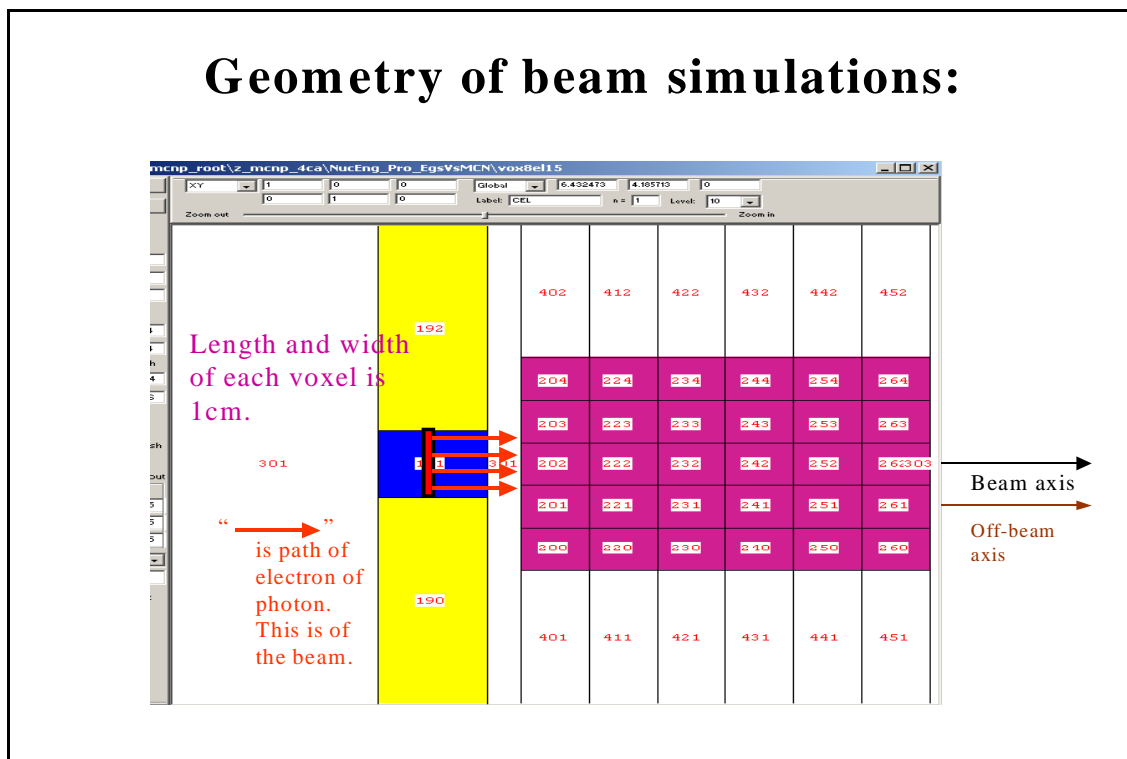


**Figure (1).** All of the cells consisting of H<sub>2</sub>O or soft tissue appear as   in Figure (1). Purple cells 202, 222, etc. have density of 1.00 gm/cm<sup>3</sup>. There 700,000 source particles.

In figure (1), note that cells 202, 222, 232, 242, 252, and 262 of Figure (1) lie directly on the axis of the beam of radiation, which emerges from inside the blue cell 101. This axis was defined as the X-axis. All of the cells consisting of H<sub>2</sub>O or soft tissue appear as   in Figure (1). These purple cells have a density of 1.00 gm/cm<sup>3</sup> and are denoted as voxels, as in the medical conventionalism.

In figure (I) and in all of the beam simulations of this paper, the beam is rectangularly shaped. The beam traverses along the X-axis. The beam has width-y of 1.6cm and width-z of 1.6cm. The beam was populated either by 700,000 monoenergetic electrons or 700,000 monoenergetic photons. The choices of energy for the initially monoenergetic were .5MeV, 1MeV, 6MeV, and finally 18MeV. These simulations were conducted with both MCNP and EGSnrc, using 700,000 source particles (e.g. nps).

This paragraph gives an example of a typical MCNP input file used to by the author in order to generate the calculation of doses of those voxels of figure (1) which are especially of interest. The doses due to MCNP were extracted by setting up the MCNP input file to have either F6 cards for MeV's per gram or \*F8 cards for MeV's of energy released per chosen type of particle in a given cell. (choice of particle to read should not change in a dosimetric file). *Appendix A* shows the typical type of MCNP file used to model delivery of dose from monoenergetic electrons to 'purple' geometry of the phantom which is described in Figure (1).

The \*F8 cards and the source cards were specially chosen for the MCNP input file for modelling the electron beam therapy of the phantom of Figure (1). The following several lines show the \*F8 cards of the input and the source card governing the generation of a 6 MeV beam of monoenergetic electrons.

```

mode e p
c the source card defined the emergence of a beam of 6MeV electrons.
sdef erg= 6.0 SUR=1312 POS=1.2 0 0 RAD=D1 DIR=1 ccc=191 PAR=3 $ ccc Means cookiCutterCell;
SI1 1.2 $ 1.2 > sqrt(2)*1/2WidtBox=sqrt(2)*.8cm. $ next:
C
F18*:p 201 221 231 241 251 261 $ energy deposited into cell ; 2nd phot/ from electrons
F28*:p 202 222 232 242 252 262 $ energy deposited into cell ; 2ndy photons
F38*:p 203 223 233 243 253 263 $ energy deposited into cell ; 2ndy photons
E0 0.050 1.0 3.0 6.0 $ energy bin splitters . .

```

### 3. NUMERICAL DATA FROM THE DOSE SIMULATIONS.

#### 3.1 Durations of Simulations

Dosimetric Results of beam Monoenergetic Electrons hitting rectangular target of “soft tissue” are given in the next tables. Note that soft tissue consists of 80% H<sub>2</sub>O and of organics. Soft tissue is equivalent to water in terms of dosimetry, attenuations, and stopping powers.

**Table I. Durations of Dose Simulations as a Function of Energy and Code.**

E of particles from beam	Simulation time via MCNP (min)	Simulation time via EGSnrc (min)	Simulation time via MCNP (min)	Simulation time via EGSnrc (min)	Simulation time via MCNP (min)
Particle of or by the beam: below: E-beam	electron (e)	electron (e)	photon (p)	photon (p)	Secondary* e's generated from p's
0.5 MeV	59.5	1.1133	0.6	0.31333	about 10
1. MeV	110.88	1.875	0.57	0.42167	21.3
6. MeV	586.18	8.955	0.54	0.90833	54
18. MeV	1425.4	17.388	0.59	1.1883	105

\* Secondary e's are consequential to stuff lost by photons.

700,000 source particles existed for the particles of the initial beam for each simulation recorded in Table I. In the last column, the results of the secondary electrons either liberated or generated by the photons are recorded. A summary of observations of the running times of the different particles as a function of energy and choice code is offered here. EGSnrc simulations of electrons are much faster than MCNP simulations of electrons, often by more than 40 fold. Plain photon simulations via MCNP are almost as fast as those of EGSnrc, so long as doses and scalar fluxes due to secondary electrons are not evaluated and computationally recorded.

It will be seen from Table Q that at energies above 1 MeV for photons, dose contributions due to secondary electrons cannot be ignored. Therefore an MCNP simulation in primary photon mode plus a 2<sup>nd</sup> MCNP simulation in the (p-e) mode should be carried out - if the photon beam energy exceeds 1 MeV. The (p)-mode simulations take only 1 minute approximately, but the (p-

e) mode simulations to include secondary electrons (e.g. p collision daughters) endure for more than 20 minutes. The times of these two distinct simulations need to be added to get the realistic duration of a complete dose simulation for beams above 1 MeV.

### 3.2 Doses to the voxels due to electron beams

In this paragraph and the next few pages, we focus on dosimetry results, on how much dose is imparted to a given voxel due to a beam of electrons here and later hard photon beams.

Numerous tables of doses generated by electron beams are given.

**Table II. Doses of Voxels which are on the Beam Axis.**

x-mcell (cm)	DosemnpElectrish [OnbeamX] (gray/disint.)	Fluctuationmnp Electrish [OnbeamX]	DoseElectrish [OnbeamX] (gray/disint.)	Fluctuation Electrish[OnbeamX] (decimal)	Ebeam (MeV)
3.	3.080000e-11	0.00171	3.7416401e-11	0.0014521	0.5
4.	0.	0	8.4273091e-16	0.1151	0.5
5.	0.	0	2.6252445e-16	0.17607	0.5
6.	0.	0	1.26143e-16	0.27086	0.5
7.	0.	0	2.5876721e-17	0.40368	0.5
8.	0.	0	0	1.	0.5
3.	6.191680e-11	0.0016004	7.5226918e-11	0.0013726	1
4.	0.	0	3.4370879e-15	0.0717	1
5.	0.	0	1.3232981e-15	0.13635	1
6.	0.	0	7.3522008e-16	0.20126	1
7.	0.	0	5.654705e-16	0.24714	1
8.	0.	0	0	1.	1
3.	3.071424e-10	0.00038631	1.5183653e-10	0.0013858	6
4.	2.213264e-10	0.00077263	1.3486142e-10	0.0015752	6
5.	6.933456e-11	0.0023731	4.9928864e-11	0.002751	6
6.	1.662784e-12	0.010982	8.8169044e-13	0.014128	6
7.	0.	0	6.5683555e-14	0.054512	6
8.	0.	0	4.3334757e-14	0.066699	6
3.	1.3653264e-10	0.0025861	1.4613965e-10	0.0014701	18
4.	1.3626128e-10	0.0023872	1.5233602e-10	0.0014438	18
5.	1.24488e-10	0.0023872	1.4021076e-10	0.0015506	18
6.	9.6056320e-11	0.0026259	1.0866666e-10	0.0018599	18
7.	6.4334560e-11	0.0031829	7.3191358e-11	0.0023833	18
8.	3.913744e-11	0.0040582	4.520590e-11	0.0031365	18

A key description to the labels in Table II is given here: /Unit (Gray/disnt) is Grays per disintegration./

X-mcell is the x coordinate of the middle of the cell which receives dose.

DosemnpElectrish[OnbeamX] is the dose imparted to the given cell (or 1cm<sup>3</sup> voxel) due to beam electrons, scattered electrons, and liberated electrons via MCNP.

DoseElectrish[OnbeamX] is the dose imparted to the given cell of 1cm<sup>3</sup> due to electrons via

EGSnrc. FluctuationmcnpElectrish[OnbeamX] is the fluctuation of the value of the MCNP generated dose. FluctuationElectrish[OnbeamX] is the fluctuation of the value of the EGSnrc generated dose. The values of fluctuation are given as decimals, not percentages. Ebeam is the energy of each original photon while it is in the original beam trajectory. In the label DosemcnpElectrish[OnbeamX], the nom. expression in brackets, [OnbeamX], indicates that voxels exposed are all centered in line with the particle beam axis.

The center of an [OnbeamX] voxel is located at  $(x,y,z) = (x-mcell, 0cm, 0cm)$  . In the label DosemcnpElectrish[OffbeamX], the nom. expression in brackets, [OffbeamX], indicates that voxels exposed are laterally centered one cm away from the particle beam axis. The center of an [OffbeamX] voxel is located at  $(x,y,z) = (x-mcell, 1cm, 0cm)$  .

**Table III. Doses of Voxels which are 1cm off-beam**

x-mcell(cm)	DosemcnpElectrish [OffbeamX] (gray/disint.)	Fluctuation mcnp Electrish[Of fbeamX]	DoseElectrish [OffbeamX] (gray/disint.)	Fluctuation Electrish[Of fbeamX]	Ebeam (MeV)
3.	9.2194400e-12	0.003808	1.11574e-11	0.003203	0.5
4.	0.	0	4.266882e-16	0.13456	0.5
5.	0.	0	2.1718938e-16	0.20684	0.5
6.	0.	0	2.104271e-16	0.30325	0.5
7.	0.	0	4.6722077e-17	0.35941	0.5
8.	0.	0	0	1.00	0.5
3.	1.855568e-11	0.0035872	2.2495524e-11	0.003042	1
4.	0.	0	2.0114871e-15	0.10827	1
5.	0.	0	9.4053665e-16	0.15866	1
6.	0.	0	7.5625754e-16	0.22162	1
7.	0.	0	3.4580439e-16	0.41496	1
8.	0.	0	1.4263875e-16	0.23503	1
3.	1.992576e-12	0.014073	4.7348459e-11	0.002974	6
4.	3.120048e-11	0.0039183	5.6711974e-11	0.002770	6
5.	2.6551520e-11	0.0040839	2.566277e-11	0.003908	6
6.	3.0429760e-13	0.023731	3.8215494e-13	0.020945	6
7.	0.	0	3.7377969e-14	0.065566	6
8.	0.	0	3.1756024e-14	0.080313	6
3.	4.1034560e-11	0.0052519	4.4027332e-11	0.003195	18
4.	4.2245440e-11	0.0047744	4.7050318e-11	0.003087	18
5.	4.23696e-11	0.0045357	4.9010101e-11	0.003044	18
6.	4.0918240e-11	0.0043765	4.7964401e-11	0.003076	18
7.	3.478544000e-11	0.0044959	4.0913062e-11	0.003343	18
8.	2.6382560e-11	0.0050131	3.0634533e-11	0.003896	18

For the sake of keeping this paper within reasonable length the numerical results of secondary photons in the MCNP simulations are not include. However a simple observation of (e-p) mode simulations of secondary photons from the electron beams is offered. The dose×volume deposited in (elec-photo) mode tends to be almost the same (slightly less than) the dose×volume deposited in electron mode in the cases of .5MeV beam and 18 MeV beam , for voxels on the beam axis. This is especially true in the cells where the journey of e is more than ½ completed.

### 3.3 Doses to the voxels due to beams of monoenergetic photons

All of the data in this text involving doses generated by radiative electrons has been recorded above. In this section and in the next section all of the calculation involve doses or energy transfer originating from beams of photons or gamma rays. In the next few tables, we focus on mono energetic beams of photons. The choices of energy of the beam are: 0.5MeV, 1MeV, 6MeV, and 18 MeV.

Q = "IV"

**Table Q. Doses due to photon beam onto the Voxels which are on the Beam Axis.**

x-mcell	DosemcnpPhotonic [OnbeamX]	DosemcnpPhotonic [OnbeamX] [fileNumber+100_ini]	DosePhotonic [OnbeamX]	FluctuationmcnpPhotonic[OnbeamX]	FluctuationPhotonic [OnbeamX]	Ebeam (MeV)
3.	1.027920E-12	1.00673120e-13	1.2302810E-12	0.0015	0.007108	0.5
4.	9.628080E-13	9.61854400e-13	1.1827622E-12	0.0016	0.007238	0.5
5.	8.861744E-13	8.47724800e-13	1.0884958E-12	0.0017	0.007553	0.5
6.	8.102192E-13	8.41809600e-13	9.8091345E-13	0.0018	0.007962	0.5
7.	7.381040E-13	6.93230400e-13	9.0259443E-13	0.0019	0.008297	0.5
8.	6.700832E-13	6.880704e-13	8.1489644E-13	0.002	0.008745	0.5
3.	1.927888e-12	1.7638400e-12	2.14209776e-12	0.0015	0.008198	1
4.	1.839616e-12	1.845744e-12	2.21444424e-12	0.0015	0.007982	1
5.	1.734608e-12	1.718752e-12	2.12395133e-12	0.0016	0.008183	1
6.	1.627424e-12	1.633792e-12	1.95102057e-12	0.0017	0.008531	1
7.	1.5209008e-12	1.518658e-12	1.86924655e-12	0.0018	0.008757	1
8.	1.419352e-12	1.406464e-12	1.73595706e-12	0.0019	0.009089	1
3.	6.834256e-12	1.851936e-12	2.31514287e-12	0.0015	0.013148	6
4.	6.70744e-12	4.36096e-12	5.50972604e-12	0.0015	0.009162	6
5.	6.56128e-12	5.201008e-12	6.46691524e-12	0.0015	0.008423	6
6.	6.406032e-12	5.179616e-12	6.46042827e-12	0.0016	0.008413	6
7.	6.247024e-12	5.082896e-12	6.33955129e-12	0.0016	0.008534	6
8.	6.088192e-12	4.851648e-12	6.06212758e-12	0.0016	0.008702	6
3.	1.673392e-11	1.4964416e-12	1.91000969e-12	0.0015	0.016501	18
4.	1.648368e-11	4.242624e-12	5.34654721e-12	0.0015	0.010714	18
5.	1.622672e-11	6.231712e-12	7.96849338e-12	0.0015	0.008661	18
6.	1.5963776e-11	7.705024e-12	9.57619066e-12	0.0016	0.007793	18
7.	1.5696896e-11	8.234368e-12	1.03401675e-11	0.0016	0.007464	18
8.	1.5427264e-11	8.54688e-12	1.06294255e-11	0.0016	0.007296	18

Here is the key to labels in Table (Q):

X-mcell is the x coordinate of the middle of the cell which receives dose.

DosemcnpPhotonic[OnbeamX] is the dose imparted to the given cell (or voxel) due to photons via MCNP.

DosemcnpPhotonic[OnbeamX] [fileNumber+100,ini] is the dose imparted to the given cell (or voxel) due to secondary e's and tertiary electrons resulting from the photons, via modelling and choice of modes in MCNP.

DosePhotonic[OnbeamX] is the dose imparted to the given cell (or vox) due to photons via EGSnrc.

FluctuationmcnpPhotonic[OnbeamX] is the fluctuation of the value of the MCNP modelled dose.

FluctuationPhotonic[OnbeamX] is the fluctuation of the value of the EGSnrc generated dose.

These labels in boxes below mirror the boxes of Table (Q), where gray/disnt means Gray/ disintegration.

x- mcell (cm)	DosemcnpPhot onic [OnbeamX] (Gray/disnt)	DosemcnpPhoto nic [OnbeamX] [fileNumber+10 0.ini]	DosePhoton ic[OnbeamX] (gray/disnt)	Fluctuationmcnp Photonic[Onbea mX]	FluctuationP hotonic [OnbeamX]	Ebea m (MeV )
---------------------	---	--	---	--	--------------------------------------	------------------------

The next two graphs in figure (2) and figure (3) visually display the dose results of Table Q.

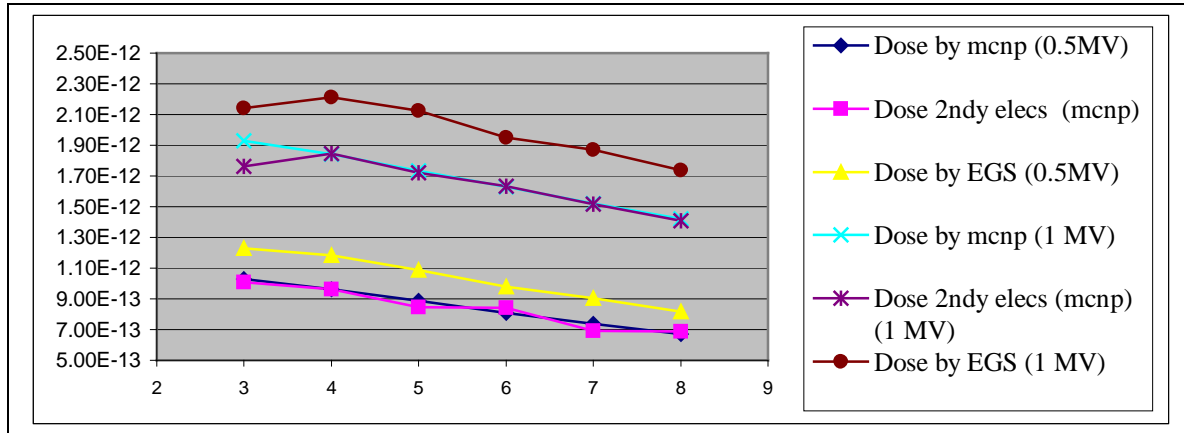


**Figure (1).** Graph of Doses from Table Q, Comparison of Doses by main photons by MCNP and Doses due to secondary mediating elec's. Beam energies are .5MeV and 1MeV.

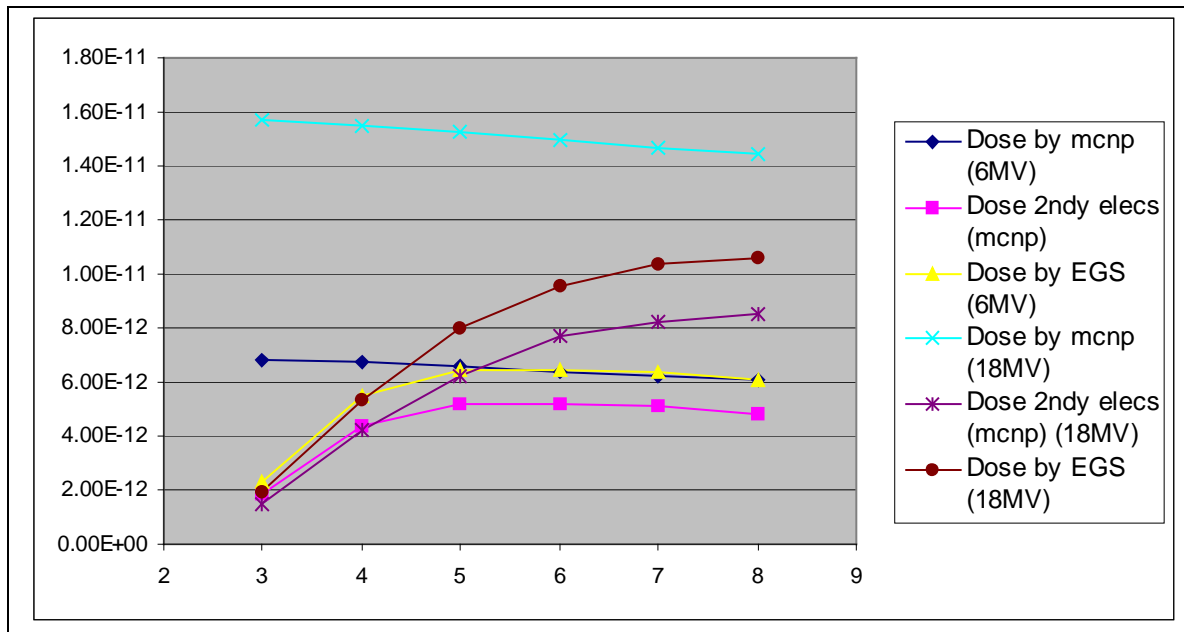


**Figure (3).** Graph of Doses from Table Q, Comparison of Doses by main photons by MCNP and Doses due to secondary mediating electrons. The two highest beam energies were selected.



Now let us consider the dose imparted to voxels which are laterally adjacent to the voxels which lie on the beam axis. The off-beam voxels which recorded in the next table include: cell 201, 221, 231, 241, 251, and 261 of figure (1). Again the dose contribution from secondary electrons is recorded in the third column of the next column, except for the case of 1MeV.

**Table V. Photonic Doses of Voxels which are 1cm away from the center of Beam Axis.**

x-mcell (cm)	DosemncnpPhotonic [OffbeamX] (Gray/disnt)	DosemncnpPhotonic [OffbeamX] [fileNumber+100_in]	DosePhotonic[OffbeamX] (Gray/disnt)	FluctuationPhotonic [OffbeamX]	FluctuationmncnpPhotonic[OffbeamX]	Ebeam (MeV)
3.	3.136016e-13	almost same	3.73969226e-13	0.0032	0.012853	0.5
4.	2.991328e-13	almost same	3.61152556e-13	0.0033	0.013053	0.5
5.	2.79496e-13	almost same	3.45025877e-13	0.0034	0.013347	0.5
6.	2.57768e-13	almost same	3.09734512e-13	0.0035	0.014072	0.5
7.	2.363424e-13	almost same	2.96630162e-13	0.0037	0.014445	0.5
8.	2.147904e-13	almost same	2.55712085e-13	0.0039	0.015543	0.5
3.	5.82672e-13	5.3605440e-14	6.65687734e-13	0.014623	0.0032	1
4.	5.63224e-13	5.6814560e-14	6.88107634e-13	0.014282	0.0033	1
5.	5.36432e-13	5.3969120e-14	6.60692535e-13	0.014483	0.0034	1
6.	5.078688e-13	4.9910720e-14	6.15087244e-13	0.014979	0.0035	1
7.	4.775472e-13	4.8464480e-14	5.88413493e-13	0.015403	0.0036	1
8.	4.460336e-13	4.4794400e-14	5.51509738e-13	0.015877	0.0037	1
3.	2.05101e-12	5.909088e-13	7.277733e-13	0.023098	0.0033	6
4.	2.01731e-12	1.541384e-12	1.858730e-12	0.01548	0.0033	6
5.	1.98061e-12	1.929008e-12	2.356338e-12	0.01383	0.0033	6
6.	1.93995e-12	1.931152e-12	2.376313e-12	0.01365	0.0034	6
7.	1.89770e-12	1.882576e-12	2.315397e-12	0.01385	0.0034	6
8.	1.85214e-12	1.8492e-12	2.234791e-12	0.014087	0.0035	6
3.	5.01861e-12	4.652624e-13	5.765945e-13	0.02934	0.0033	18
4.	4.94698e-12	1.4620208e-12	1.713444e-12	0.01841	0.0033	18
5.	4.87256e-12	2.2312e-12	2.674482e-12	0.014544	0.0033	18
6.	4.79757e-12	2.559152e-12	3.426078e-12	0.01275	0.0034	18
7.	4.72142e-12	3.120976e-12	3.913567e-12	0.01184	0.0034	18
8.	4.64566e-12	3.454656e-12	4.161854e-12	0.01139	0.0034	18

As with the other dose tables the initial energy of primary photon (i.e. Ebeam) equals .5, 1, 6, or 18 MeV.

Next we consider a point source of photonic Cs-137 surrounded by soft tissue or water. Consider good agreement between photon simulations of MCNP and EGS for spherical phantom with 18 cm diameter. A point source or microscopic cubic source containing highly concentrated Cs-137 is placed in the center of the spherical phantom. Note that EGS geometry mimics an approximate sphere with numerous rectangular cells of H<sub>2</sub>O.

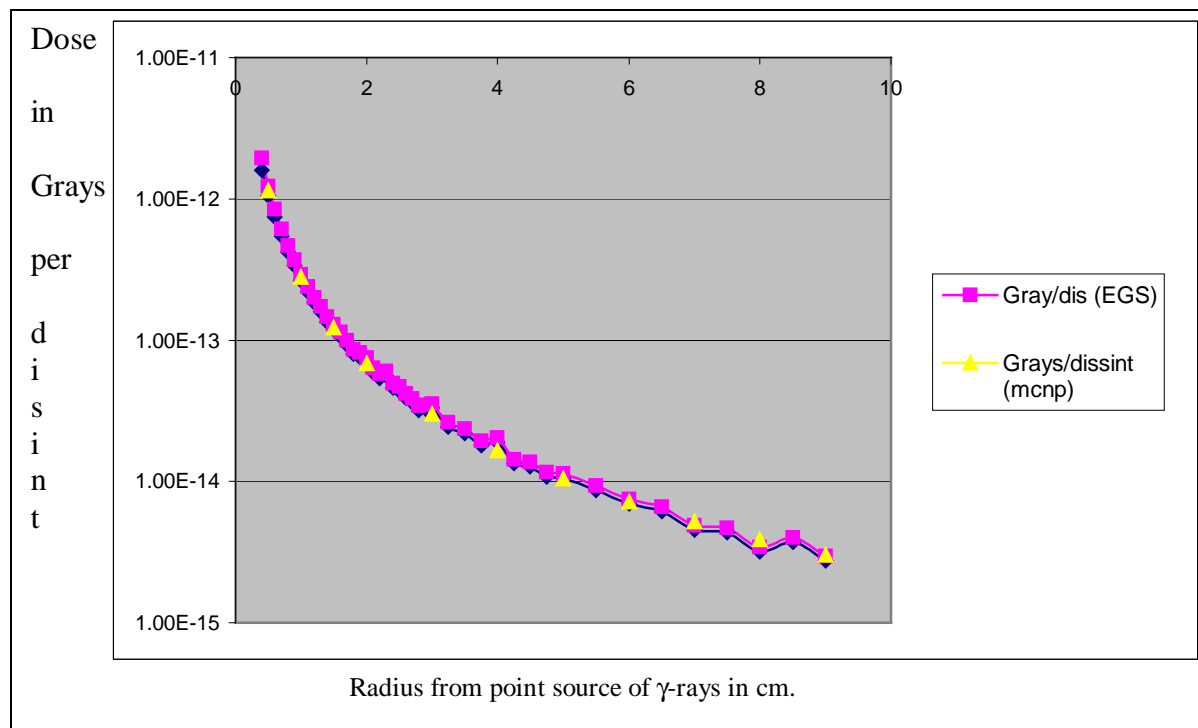


**Figure (4). Dose per disintegration ('disint') versus r from Cs-137 source in H<sub>2</sub>O.**

### 3. CONCLUSIONS

From preliminary review it is clear that EGSnrc is much faster than MCNP at modelling primary electrons. MCNP is more versatile than EGSnrc. Only dose and fluctuations are recorded by EGSnrc. Based on the understanding of differences, it is expected that not any time within the span of several years will EGSnrc be modified to include protons for proton therapy. EGSnrc internally is most reliable for rectangular geometries.

EGSnrc can read spectra and geometry and compositions from external files. - contributing to convenience. MCNP when specialized can read external geometry. The (p-e) mode simulations of photons should be done within MCNP in addition to the (p) mode simulation. A study of the dose tables herein makes this clear.

Conclusive statements: A thorough study of the tables given for the dosimetry of photon targeted Figure (1) makes it very apparent that the dose values in (p-e) mode of MCNP are almost consistently closer to the dose values in (p)mode of EGSnrc than the values of the (p) mode simulations of MCNP. Moreover, the dose distributions as a function of beam depth from EGSnrc and MCNP in (p-e) mode match the dosimetric beam profiles given in the graphs of the text The Physics of Radiation Therapy [2]. On the other hand, the dose distribution by MCNP simulation in purely (p) mode fails to account for significant build up and the graphs published in Kahn's book. The agreement between the dose table of values from MCNP's (p-e) mode and the values of EGSnrc are reasonably close. The patterns of the graphs of MCNP's (p-e) mode the corresponding graphs of EGSnrc are very close, such that the ratio of the two graphs remains constant, although not exactly equal to one.

## REFERENCES

1. Code EGSnrc; Ionizing Radiation Standards; national research council of Canada; <http://www.irs.inms.nrc.ca/>; (2006-7).
2. Faiz Kahn, The Physics of Radiation Therapy (Third Ed.), pg. 163, (2003).
3. Frank Attix, Introduction to Radiological Physics and Radiation Dosimetry, pg. 229, Wiley-Interscience (USA), (1987). Page 229 has a photon dose graph.

## APPENDIX A

c new tool in 2007 on cyl cookie cutter Makng sqr. Erg electr= 6MeV  
c 2 1 -1.000 302 -303 501 -502 801 -802 \$ 1702; targ flesh  
200 1 -1.000 302 -303 501 -502 801 -901 imp:e 1 \$ 1702; targ flesh  
201 1 -1.000 302 -303 501 -502 901 -1021 imp:e 1 \$ 1702; targ flesh  
202 1 -1.000 302 -303 501 -502 1021 -1022 imp:e 1 \$ 1702; targ flesh  
203 1 -1.000 302 -303 501 -502 1022 -902 imp:e 1 \$ 1702; targ flesh  
204 1 -1.000 302 -303 501 -502 902 -802 imp:e 1 \$ 1702; targ flesh  
220 1 -1.000 303 -304 501 -502 801 -901 imp:e 1 \$ targ flesh  
221 1 -1.000 303 -304 501 -502 901 -1021 imp:e 1 \$ targ flesh  
222 1 -1.000 303 -304 501 -502 1021 -1022 imp:e 1 \$ targ flesh  
223 1 -1.000 303 -304 501 -502 1022 -902 imp:e 1 \$ targ flesh  
224 1 -1.000 303 -304 501 -502 902 -802 imp:e 1 \$ targ flesh  
230 1 -1.000 304 -305 501 -502 801 -901 imp:e 1 \$ targ flesh  
231 1 -1.000 304 -305 501 -502 901 -1021 imp:e 1 \$ targ flesh  
232 1 -1.000 304 -305 501 -502 1021 -1022 imp:e 1 \$ targ flesh  
233 1 -1.000 304 -305 501 -502 1022 -902 imp:e 1 \$ targ flesh  
234 1 -1.000 304 -305 501 -502 902 -802 imp:e 1 \$ targ flesh  
240 1 -1.000 305 -306 501 -502 801 -901 imp:e 1 \$ targ flesh  
241 1 -1.000 305 -306 501 -502 901 -1021 imp:e 1 \$ targ flesh  
242 1 -1.000 305 -306 501 -502 1021 -1022 imp:e 1 \$ targ flesh  
243 1 -1.000 305 -306 501 -502 1022 -902 imp:e 1 \$ targ flesh  
244 1 -1.000 305 -306 501 -502 902 -802 imp:e 1 \$ targ flesh  
250 1 -1.000 306 -307 501 -502 801 -901 imp:e 1 \$ targ flesh  
251 1 -1.000 306 -307 501 -502 901 -1021 imp:e 1 \$ targ flesh  
252 1 -1.000 306 -307 501 -502 1021 -1022 imp:e 1 \$ targ flesh  
253 1 -1.000 306 -307 501 -502 1022 -902 imp:e 1 \$ targ flesh  
254 1 -1.000 306 -307 501 -502 902 -802 imp:e 1 \$ targ flesh  
260 1 -1.000 307 -308 501 -502 801 -901 imp:e 1 \$ targ flesh  
261 1 -1.000 307 -308 501 -502 901 -1021 imp:e 1 \$ targ flesh  
262 1 -1.000 307 -308 501 -502 1021 -1022 imp:e 1 \$ targ flesh  
263 1 -1.000 307 -308 501 -502 1022 -902 imp:e 1 \$ targ flesh  
264 1 -1.000 307 -308 501 -502 902 -802 imp:e 1 \$ targ flesh  
c  
c Shift in z coordinate by -1 centimeter:  
1200 1 -1.000 302 -303 1501 -501 801 -901 imp:e 1 \$ 1702; targ flesh

1201 1 -1.000 302 -303 1501 -501 901 -1021 imp:e 1 \$ 1702; targ flesh  
1202 1 -1.000 302 -303 1501 -501 1021 -1022 imp:e 1 \$ 1702; targ flesh  
1203 1 -1.000 302 -303 1501 -501 1022 -902 imp:e 1 \$ 1702; targ flesh  
1204 1 -1.000 302 -303 1501 -501 902 -802 imp:e 1 \$ 1702; targ flesh  
c this is a parallel planar repetition of cell 204  
1220 1 -1.000 303 -304 1501 -501 801 -901 imp:e 1 \$ targ flesh  
c this is a parallel planar repetition of cell 220  
1221 1 -1.000 303 -304 1501 -501 901 -1021 imp:e 1 \$ targ flesh  
c this is a parallel planar repetition of cell 221  
1222 1 -1.000 303 -304 1501 -501 1021 -1022 imp:e 1 \$ targ flesh  
c this is a parallel planar repetition of cell 222  
1223 1 -1.000 303 -304 1501 -501 1022 -902 imp:e 1 \$ targ flesh  
c this is a parallel planar repetition of cell 223  
..... cells 1224 through 1264 have been omitted from this reproduction in Appdx. A.  
c  
c Shift in z coordinate by +1 centimeter:  
2200 1 -1.000 302 -303 502 -1502 801 -901 imp:e 1 \$ 1702; targ flesh  
c this is a parallel planar repetition of cell 1200  
2201 1 -1.000 302 -303 502 -1502 901 -1021 imp:e 1 \$ 1702; targ flesh  
c this is a parallel planar repetition of cell 2200  
2202 1 -1.000 302 -303 502 -1502 1021 -1022 imp:e 1 \$ 1702;targ flesh  
c this is a parallel planar repetition of cell 2202  
..... cells 2203 through 2264 have been omitted from this reproduction in Appdx. A.  
c  
401 0 302 -303 1501 -1502 -801 -900 imp:e 1 \$//correctd  
402 0 302 -303 1501 -1502 802 -900 imp:e 1 \$//correctd  
411 0 303 -304 1501 -1502 -801 -900 imp:e 1 \$//correctd  
412 0 303 -304 1501 -1502 802 -900 imp:e 1  
421 0 304 -305 1501 -1502 -801 -900 imp:e 1  
422 0 304 -305 1501 -1502 802 -900 imp:e 1  
431 0 305 -306 1501 -1502 -801 -900 imp:e 1  
432 0 305 -306 1501 -1502 802 -900 imp:e 1  
441 0 306 -307 1501 -1502 -801 -900 imp:e 1 \$//correctd  
442 0 306 -307 1501 -1502 802 -900 imp:e 1  
451 0 307 -308 1501 -1502 -801 -900 imp:e 1  
452 0 307 -308 1501 -1502 802 -900 imp:e 1  
c These were equatorial cells  
191 3 -0.000002 -4 401 -402 imp:e 1 \$ cell whence beam emerges  
190 5 -0.000001 -4 -401 -900 imp:e 1  
192 5 -0.000001 -4 402 -900 imp:e 1  
c These were equatorial cells;  
c 301 0 4 -302 -900 501 -502 imp:e 1  
301 0 4 -302 -900 1501 -1502 imp:e 1  
303 0 4 308 -900 1501 -1502 imp:e 1 \$ 30\* boundry incrses  
c  
c removed from target cell; 1702 1 -1.000 -1702  
c  
c 51 5 -0.000001 -1501 -900 imp:e 1 \$ australZ sphere  
c 52 5 -0.000001 1502 -900 imp:e 1 \$ borealZ sphere  
51 0 -1501 -900 imp:e 1 \$ australZ sphere  
52 0 1502 -900 imp:e 1 \$ borealZ sphere

9000 0 900 imp:e 0

c surface cards

4 c/y 1.2 0.0 0.8

1702 s 5.0 0.0 0 1.0 \$ lastN is radius

c

302 px 2.5

303 px 3.5

304 px 4.5

305 px 5.5

306 px 6.5

307 px 7.5

308 px 8.5

c

401 py -0.8

402 py 0.8

c 801 py -1.50

801 py -2.50

901 py -1.50

902 py 1.50

802 py 2.50

c

1022 py 0.50

1021 py -0.50

c

1501 pz -1.50

1502 pz 1.50

501 pz -0.50

502 pz 0.50

c

1312 px -5.0 \$ plane of beam emergence

900 s 0 0 0 15

mode e p

c the source card defined the emergence of a beam of 6MeV electrons.

sdef erg= 6.0 SUR=1312 POS=1.2 0 0 RAD=D1 DIR=1 ccc=191 PAR=3 \$ ccc Means cookiCutterCell;

SII 1.2 \$ 1.2 > sqrt(2)\*1/2WidtBox=sqrt(2)\*.8cm.

C next:

F18\*:p 201 221 231 241 251 261 \$ 2nd phot ; electrish/ from electrons

F28\*:p 202 222 232 242 252 262 \$ 2ndy photons ; electrish

F38\*:p 203 223 233 243 253 263 \$ 2ndy photons ; electrish

E0 0.050 1.0 3.0 6.0 \$ energy bin splitters

m1 01001 .667 08016 .333 \$ mass composition type 1

c m1 could be replaced by biological soft tissue composition.

m3 01001 .07 06012 .2 05000 .8 \$ mass composition type 3

m5 06012 1.0

nps 700000 \$ # of source particles released for simulation